4-th International Meeting on
Cavitation and Dynamic Problems in Hydraulic Machinery and Systems,
October, 26-28, 2011, Belgrade, Serbia

Simulation of Water Hammer Induced Column Separation through Electrical Analogy

Christophe NICOLET[1], Timothy KAELBEL[2], Sébastien ALLIGNE[2], Nicolas RUCHONNET[2], Philippe ALLENBACH[3], Anton BERGANT[4], François AVELLAN[2]

[1]Power Vision Engineering sàrl, Ch. des Champs-Courbes 1, CH-1024 Ecublens, Switzerland,
christophe.nicolet@powervision-eng.ch
[2]Laboratory for Hydraulic Machines, Ecole Polytechnique Fédérale de Lausanne, EPFL
Av. de Cour 33bis, CH-1007 Lausanne, Switzerland,
timothy.kaelbel@epfl.ch, sebastien.alligne@epfl.ch, nicolas.ruchonnet@epfl.ch, francois.avelllan@epfl.ch
[3]Laboratory of Electrical Machines, Ecole Polytechnique Fédérale de Lausanne, EPFL
CH-1015 Lausanne, Switzerland, philippe.allenbach@epfl.ch
[4]Litostroj Power d.o.o., Litostrojska 50, 1000 Ljubljana, Slovenia, anton.bergant@litostrojpower.eu

Abstract

This paper presents the modeling, simulation and related validation of water column separation in hydraulic systems. First, the modeling of hydraulic components using electrical analogy is introduced. This modeling is based on finite difference method with a centered scheme in space and Lax scheme for discharge applied to momentum and continuity equations in case of a pipe filled with fluid. The resulting set of ordinary differential equations can be represented as a T-shaped electrical equivalent scheme. The possible thermodynamic damping of fluid and pipe material is also introduced and the equivalent scheme is adapted consequently. The time domain numerical integration of the equation set is performed using Runge-Kutta fourth order method. Then, the model of water column separation is presented. This model assumes an initial free gas content homogeneously distributed leading to a wave speed in pipe with liquid – free gas mixture which is strongly pressure dependent. The water column model is implemented in the simulation software SIMSEN and validated for a case of water column separation induced by water hammer. The test case is a pipe connected upstream to a constant pressure reservoir and downstream to a valve which sudden closure induces water hammer with water column separation occurring during the rarefaction phase. The comparison between simulation results and measurements show good agreement for two different sets of initial conditions if appropriate set of parameters is used. Finally, a parametric study is presented to show the influence of the minimum wave speed value and of the thermodynamic damping.

Keywords: Water column separation, water hammer, fluid transients in pipes.

1. Introduction

Water hammer negative pressure waves induced by hydraulic systems transients may lead to column separation when the pressure drops to the liquid vapour pressure. The sudden pressure rise resulting from the vapour cavity collapse is a severe loading for the hydraulic system structure, jeopardizing the system integrity. Therefore, water column separation was extensively studied experimentally and numerically, see Bergant *et al.* [1]. The method of characteristics, MOC, is extensively used to address the water column separation where this phenomenon can be modeled with several different approaches, see Wylie and Streeter [2]. Among them, the Discrete Gas Cavity Model, DGCM, has proven to be very effective and is widely used in industrial numerical simulation software. However, the finite difference methods are less commonly used to simulate water column separation. Thus, this paper presents the modeling, simulation and validation of a water column separation model based on homogenous free gas mixture implemented in the simulation software SIMSEN. The modeling of hydraulic components in SIMSEN is made through electrical analogy where pressurized cavitation free pipes are modeled by a T-shaped equivalent circuit resulting from finite difference numerical scheme. This model has been extended to water column separation by introducing the wave speed pressure and initial free gas void fraction dependency and by introducing a thermodynamic damping. Simulation results obtained with this Free Gas Mixture Model are compared with simulation results obtained with MOC-DGCM and with experiments.

2. Hydroacoustic modeling through electrical analogy

2.1 Fundamental equations and numerical scheme

The momentum and continuity equations derived for an elementary pipe of a length *dx*, see Fig. 1 left, neglecting the convective terms $C\partial/\partial x$ and assuming plane pressure wave and uniform velocity field in a cross section, lead to the following set of hyperbolic partial differential equations, see Wylie and Streeter [2]:

$$\begin{cases} \dfrac{\partial h}{\partial x} + \dfrac{1}{gA}\dfrac{\partial Q}{\partial t} + \dfrac{\lambda Q|Q|}{2gDA^2} = 0 \\ \dfrac{\partial h}{\partial t} + \dfrac{a^2}{gA}\dfrac{\partial Q}{\partial x} = 0 \end{cases} \tag{1}$$

Where the h and Q variables are the piezometric head and the discharge, respectively. Introducing hydraulic resistance R', inductance L' and capacitance C' (Paynter [3]) equation set (1) can be reformulated as:

$$\begin{cases} \dfrac{\partial h}{\partial x} + L'\dfrac{\partial Q}{\partial t} + R'(Q)|Q| = 0 \\ \dfrac{\partial h}{\partial t} + \dfrac{1}{C'}\dfrac{\partial Q}{\partial x} = 0 \end{cases} \tag{2}$$

The system of hyperbolic equations (2) is solved using Finite Difference Method considering a 1st order centered scheme discretization in space and a Lax scheme for the discharge, see Nicolet [4]:

$$\left.\frac{\partial Q}{\partial x}\right|_{i+1/2} = \frac{Q_{i+1} - Q_i}{dx} \qquad \left.\frac{\partial h}{\partial x}\right|_{i+1/2} = \frac{h_{i+1} - h_i}{dx} \qquad Q_{i+1/2} = \frac{Q_{i+1} + Q_i}{2} \tag{3}$$

This approach leads to a system of ordinary differential equations that can be represented as a T-shaped equivalent scheme as presented in Fig. 1 right. The RLC parameters of this equivalent scheme early deduced by Paynter [3] are given by:

$$R = \frac{\lambda|Q|dx}{2gDA^2} \qquad L = \frac{dx}{gA} \qquad C = \frac{gAdx}{a^2} \tag{4}$$

Here λ is the friction coefficient. The hydraulic resistance *R*, inductance *L* and capacitance *C* correspond respectively to friction losses, inertia and storage effects. The equation set associated with the equivalent electrical scheme of Fig. 1 right, can be written with matrix formalism:

$$\begin{bmatrix} C & 0 & 0 \\ 0 & L/2 & 0 \\ 0 & 0 & L/2 \end{bmatrix} \cdot \frac{d}{dt}\begin{bmatrix} h_{i+1/2} \\ Q_i \\ Q_{i+1} \end{bmatrix} + \begin{bmatrix} 0 & -1 & 1 \\ 1 & R/2 & 0 \\ -1 & 0 & R/2 \end{bmatrix} \cdot \begin{bmatrix} h_{i+1/2} \\ Q_i \\ Q_{i+1} \end{bmatrix} = \begin{bmatrix} 0 \\ h_i \\ -h_{i+1} \end{bmatrix} \tag{5}$$

Where h_i and h_{i+1} are boundary conditions of pressure.

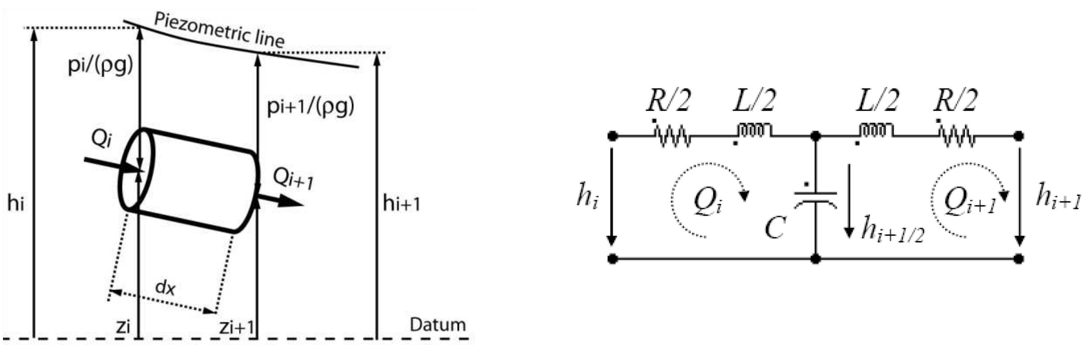

Fig. 1 Equivalent scheme of a pipe

The model of elementary pipe is extended to a whole pipe of length *l* by discretizing the pipe in *n* element and thus combing *n* electrical equivalent schemes in series as illustrated in Fig. 2.

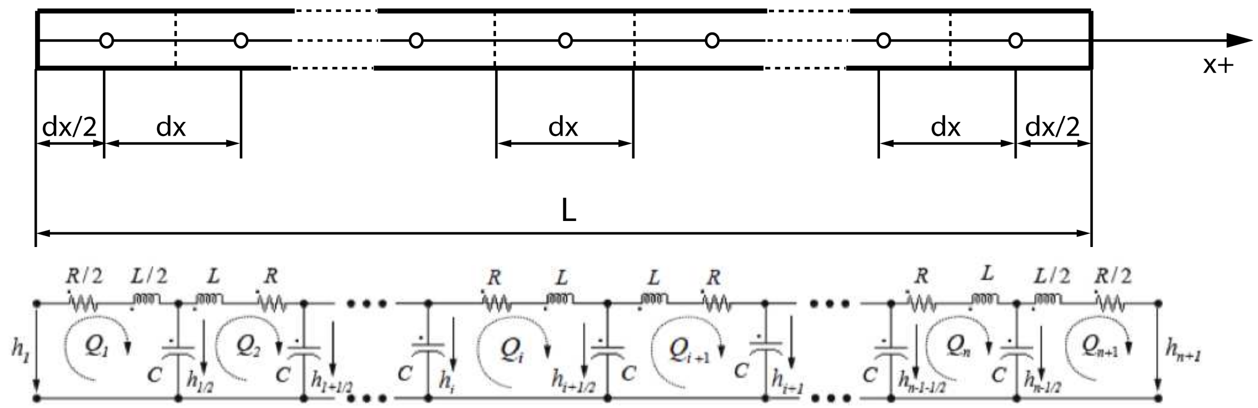

Fig. 2 Equivalent scheme of a whole pipe disctretized in "*n*" elements

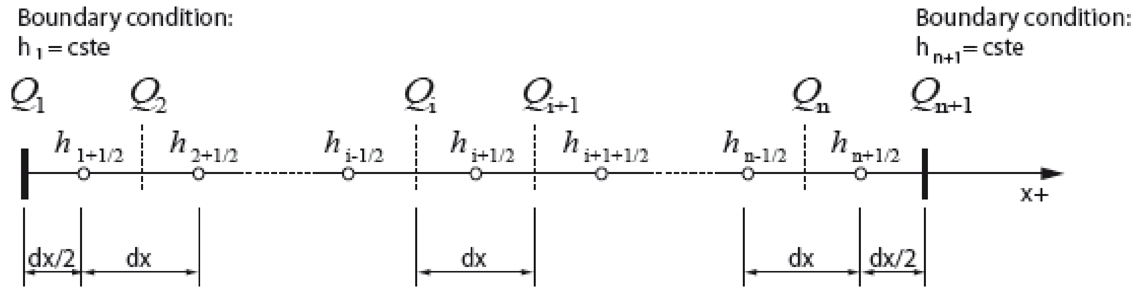

Fig. 3 Spatial distribution of state variables of the pipe model, i.e. discharges *Q* and piezometric heads *h*

The simulation models of hydraulic components based on equivalent scheme representation are implemented in the simulation software SIMSEN developed by EPFL, [4]. In this software, the system of equations is set-up using Kirchoff laws and time integration of the full system is achieved by a Runge-Kutta 4th order procedure. The simulation software SIMSEN also includes the models of all classical hydraulic components such as valves, surge tanks, surge vessels, Francis pump-turbine, Pelton and Kaplan turbines, pumps, etc, [4], [5].

2.2 Homogenous bubbly-fluid mixture

The free gas content of water significantly reduces the wave speed in pressurized pipes, see [1], [6] and [7]. Wylie [6] derived wave speed in homogenous liquid free gas mixture characterized by an initial void fraction α_o defined for a reference absolute pressure p_o and leads to the following equation:

$$a = \frac{a_o}{\sqrt{1 + \frac{p_o \alpha_o a_o^{\,2}}{\rho g^2 (h - Z - Hv)^2}}} \tag{6}$$

Where :

a_0	[m/s]	Wave speed in liquid
p_0	[Pa]	Reference absolute pressure
α_0	[-]	Initial void fraction
ρ	[kg/m^3]	Liquid density
g	[m/s^2]	Gravitational acceleration
h	[m]	Piezometric head
Z	[m]	Pipe elevation
Hv	[m]	Vapour pressure head

Thus, the wave speed in liquid gas mixture is function of the local piezometric head. Figure 4 shows the wave speed evolution as function of the absolute gas partial pressure (*h-Z-Hv*) and of the initial void fraction α_o. The non-linear equation (6) is introduced in the equation set (5) for time domain simulation so that the wave speed is local piezomtric head dependant $a=a(h_i)$, similar to Himr and Haban [8]. During water column separation, the local pieometric head drops to very low values and if the local pressure becomes negative due to numerical inaccuracy, the equation (6) leads to an increase of the wave speed, see Fig. 4 left. Therefore, the wave speed is bounded to a minimum value defined as “a_{min}” as presented in Fig. 4 right to avoid numerical instability. The minimum wave speed “a_{min}” being defined *a priori*.

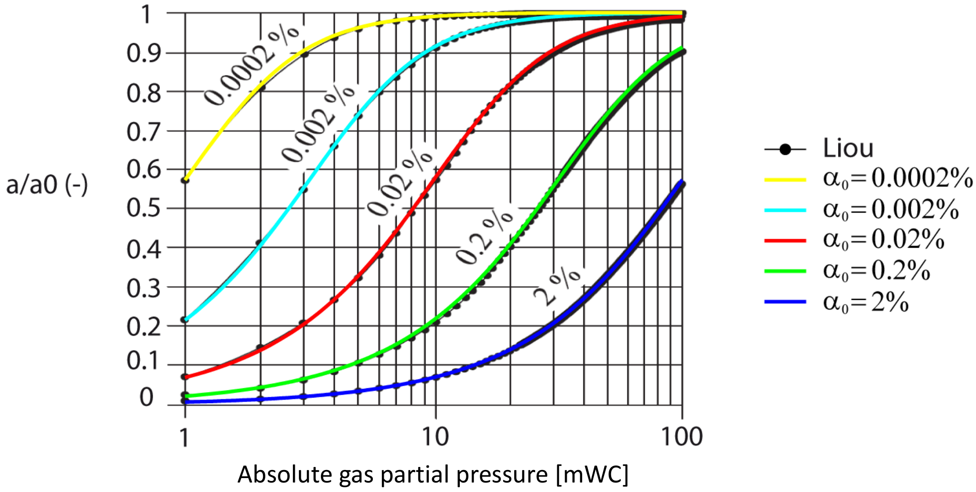

Fig. 4 Wave speed ratio as function of the initial void fraction α_o and of the absolute gas partial pressure (*h-Z-Hv*) (adapted from Liou [6])

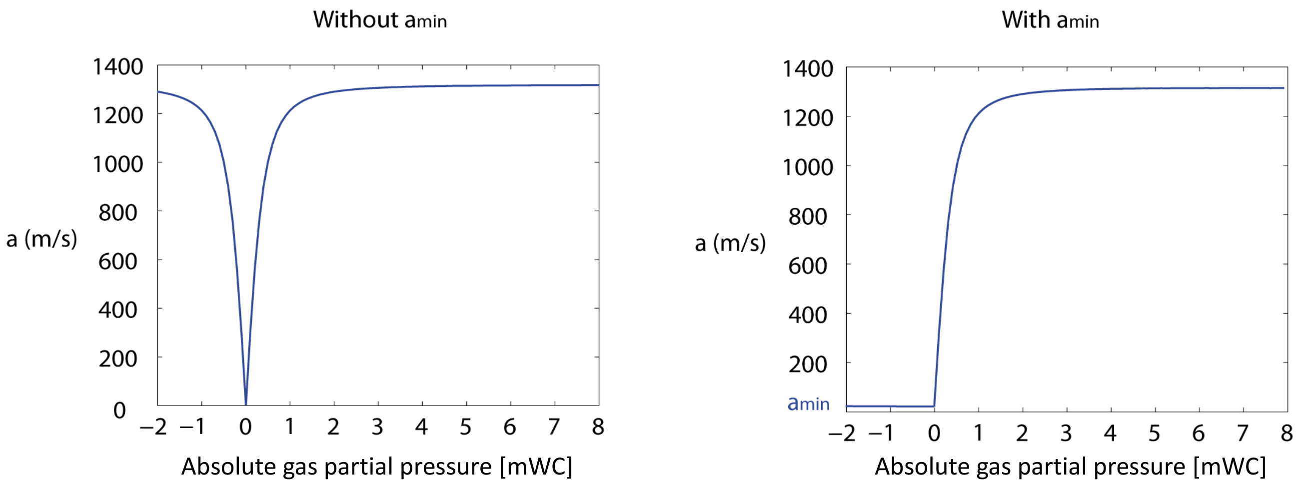

Fig. 5 Wave speed computed for α_o=10^{-7} without limitation (left) and with limitation for negative pressure (right)

2.3 Thermodynamic damping

During water column separation, the bubbly liquid vapor mixture is subjected to dissipation resulting from phase changes. This dissipation is modeled by a thermodynamic damping μ’’ also known as the bulk viscosity or fluid second viscosity, see Pezzinga [9]. This thermodynamic damping is introduced in the numerical scheme by means of an additional thermodynamic resistance R_{th} in series with the capacitance, see Allig né *et al.* [10], and defined as follows:

$$R_{th} = \frac{\mu''}{A\rho g dx} \qquad (7)$$

Pezzinga also introduced the pressure dependency of the bulk viscosity, which is not considered in this investigation and is taken as constant. The capacitance modeling the compressibility and wall deformation effects in series with thermodynamic resistance corresponds to a Kelvin-Voigt rheological model, see Fig. 6. The modified equivalent scheme of an elementary pipe with water column separation is presented in Fig. 7 with the related set of matrix equations given by equation (8).

Model	Rheologic model	Equivalent scheme	Equations
Kelvin-Voigt	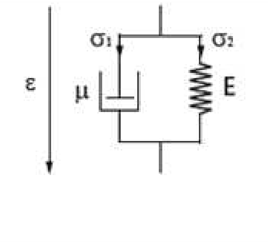	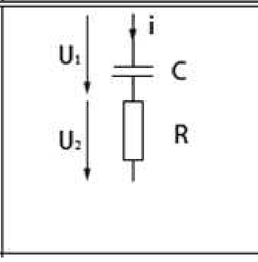	$\sigma = \sigma_1 + \sigma_2 = \varepsilon \cdot E + \mu \cdot \frac{d\varepsilon}{dt}$ $U = U_1 + U_2 = \frac{1}{C}\int i \cdot dt + R \cdot i$

Fig. 6 Rheologic Kelvin-Voigt model and related equivalent scheme

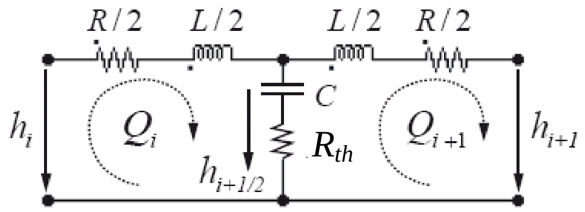

$C{=}C(a(h_{i+1/2}(t)))$

Fig. 7 Equivalent scheme of an elementary pipe with water column separation including pressure dependency of the wave speed and thermodynamic damping

$$\begin{bmatrix} C & 0 & 0 \\ 0 & L/2 & 0 \\ 0 & 0 & L/2 \end{bmatrix} \cdot \frac{d}{dt} \begin{bmatrix} h_{i+1/2} \\ Q_i \\ Q_{i+1} \end{bmatrix} + \begin{bmatrix} 0 & -1 & 1 \\ 1 & R/2 + R_{th} & -R_{th} \\ -1 & -R_{th} & R/2 + R_{th} \end{bmatrix} \cdot \begin{bmatrix} h_{i+1/2} \\ Q_i \\ Q_{i+1} \end{bmatrix} = \begin{bmatrix} 0 \\ h_i \\ -h_{i+1} \end{bmatrix} \tag{8}$$

3. Method of Characteristics and Discrete Gas Cavity Model (DGCM)

The mass of distributed free gas can be lumped at computational sections in the method of characteristics (MOC) numerical scheme leading to a discrete gas cavity model (Wylie 1984 [6]). A liquid phase with a constant wave speed *a* is assumed to occupy the computational reach. The discrete gas cavity at each internal computational section is described by the water hammer compatibility equations, the continuity equation for the gas cavity volume, and the ideal gas equation and their numerical form within the staggered grid of the method of characteristics is:

- compatibility equation along the C^+ characteristic line ($\Delta x/\Delta t = a$):

$$h_{i,t} - h_{i-1,t-\Delta t} + \frac{a}{gA}((Q_u)_{i,t} - Q_{i-1,t-\Delta t}) + \frac{f\Delta x}{2gDA^2}(Q_u)_{i,t}\left|Q_{i-1,t-\Delta t}\right| = 0 \tag{9}$$

- compatibility equation along the C^- characteristic line ($\Delta x/\Delta t = -a$):

$$h_{i,t} - h_{i+1,t-\Delta t} - \frac{a}{gA}(Q_{i,t} - (Q_u)_{i+1,t-\Delta t}) - \frac{f\Delta x}{2gDA^2}Q_{i,t}\left|(Q_u)_{i+1,t-\Delta t}\right| = 0 \tag{10}$$

- continuity equation for the gas cavity volume:

$$(V_g)_{i,t} = (V_g)_{i,t-2\Delta t} + ((1-\psi)(Q_{i,t-2\Delta t} - (Q_u)_{i,t-2\Delta t}) + \psi(Q_{i,t} - (Q_u)_{i,t}))2\Delta t \tag{11}$$

- ideal gas equation:

$$\left(V_g\right)_{i,t}(h_{i,t} - Z_i - H_v) = (h_0 - Z_0 - H_v)\alpha_0 A_i \Delta x \tag{12}$$

where i = node number, Q = node downstream-end discharge, Q_u = node upstream-end discharge, Δt = MOC time step, Δx = MOC space step, V_g = discrete cavity volume, and ψ = weighting factor. The DGCM model can be successfully used for simulation of vaporous cavitation by utilizing a low gas void fraction ($\alpha_g \leq 10^{-7}$; Wylie [4]). In this case, when the discrete cavity volume calculated by the equation (11) is negative, then the cavity volume is recalculated by equation (12). The inclusion of unsteady skin friction in DGCM improves numerical results (Bergant *et al*. [11]). Covolution-based unsteady skin friction model (Zielke [12]) is used for simulations in this paper.

4. Test Case

The test case considered here has been set-up by Bergant and Simpson, see [13], and is made of an upper pressurized reservoir (Tank 2), feeding a pipe of copper of 37.23 meters long and inner diameter of 0.0221meter, and a fast closing ball valve connected to a downstream end pressurized reservoir (Tank 1), see Fig. 8. The ball valve closure time is shorter than the pipe reflection time $2l/a$ and thus produces a direct water hammer inducing a water column separation during the rarefaction phase. Two sets of initial conditions corresponding to two different downstream counter pressures are considered and lead to initial flow velocities of C_0=0.3 m/s and C_0=1.4 m/s, respectively. The resulting pressure fluctuations induced by water hammer and water column separation are measured with a sampling frequency of 5 kHz in the midpoint of the pipe H_{mp}, and at the downstream end in front of the valve H_{ve}.

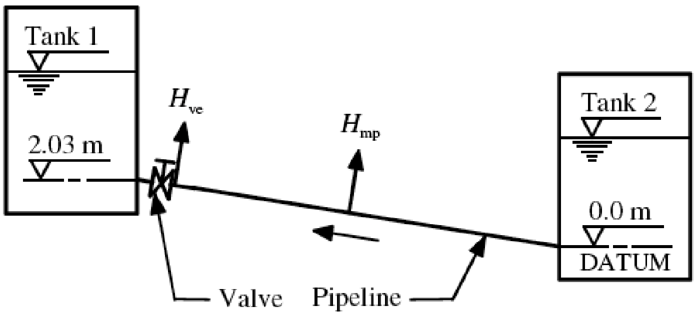

Fig. 8 Test case experimental apparatus, from [13]

Table 1 Characteristics of the experimental apparatus of Fig. 8.

Quantity	Value	Unit
Pipe length:	37.23	[m]
Pipe diameter:	0.0221	[m]
Thickness of wall pipe:	0.0016	[m]
Pipe slope:	3.2	[°]
Head in Tank 2:	22	[m]
Initial air void fraction:	10^{-7}	[-]
Valve closure time:	0.009	[s]
Wave speed in liquid:	1319	[m/s]

5. Simulation results

Time domain simulation of the fast closure of the ball valve are carried out with the simulation software SIMSEN including the water column separation model described in chapter 2 and with the MOC-DGCM method described in chapter 3. For SIMSEN simulations, the pipe is descritized with n=65 elements, with a minimum wave speed set to a_{min}=20m/s, an initial void fraction of $\alpha_o=10^{-7}$, and a thermodynamic damping set constant to $\mu=1.5\cdot10^4$ Pa·s. For MOC-DGCM numerical simulation N=64 reaches are considered with a weighting factor of ψ=1 and an initial void fraction of $\alpha_o=10^{-7}$. Simulations results obtained with the two models are compared with experimental results for the midpoint pressure H_{mp} and the pressure at the downstream valve H_{ve} for the two initial flow velocities of C_0=0.3 m/s and C_0=1.4 m/s, respectively in Fig. 9 and Fig. 10. The parameters of the Free Gas Mixture model implemented in SIMSEN were optimized to obtain a good fit with experiments. The results show good agreement in terms of maximum amplitudes and of the general shape of pressure fluctuations resulting from the water column separation. However, it could be noticed that the minimum of relative pressure of -9.8mWC below the atmospheric pressure is not imposed in the Free gas Mixture model but results from very low wave speed occurring during the rarefaction phase. Thus, the minimum pressure goes slightly below the vapor pressure and justifies the use of a minimum wave speed value a_{min}. This is not the case with the MOC-DGCM model that imposes the minimum pressure to the vapor pressure. Moreover, the simulation results presented over 1.5s in Fig. 11, shows that the Free Gas Mixture model features a frequency difference with experiments which depends on the selection of the values of a_{min} and of the thermodynamic damping. Moreover, this simulation does not account for unsteady friction model and thus the damping of the pressure fluctuations of this model is lower than in experiments for the case at C_0=1.3m/s while the

MOC-DGCM shows a very good agreement on the damping over long term transient. The MOC-DGCM model does include unsteady friction term.

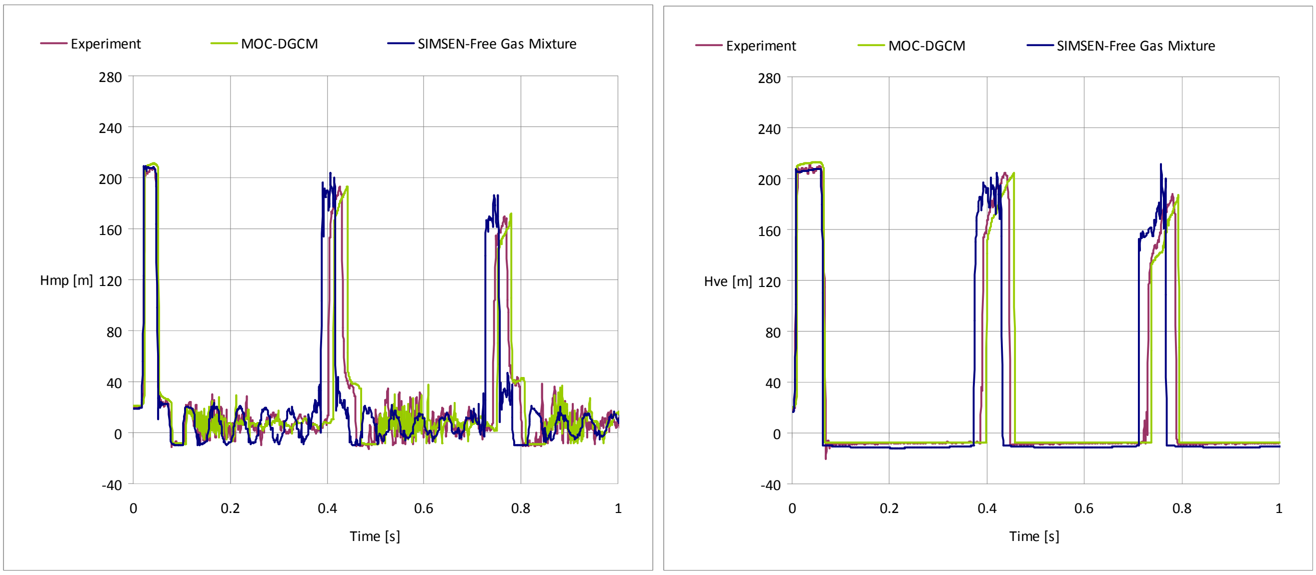

Fig. 9 Comparison simulation results obtained with SIMSEN free-gas mixture model and MOC-DGCM model with experimental results for C_0=1.4 m/s at the midpoint (left) and downstream valve (right)

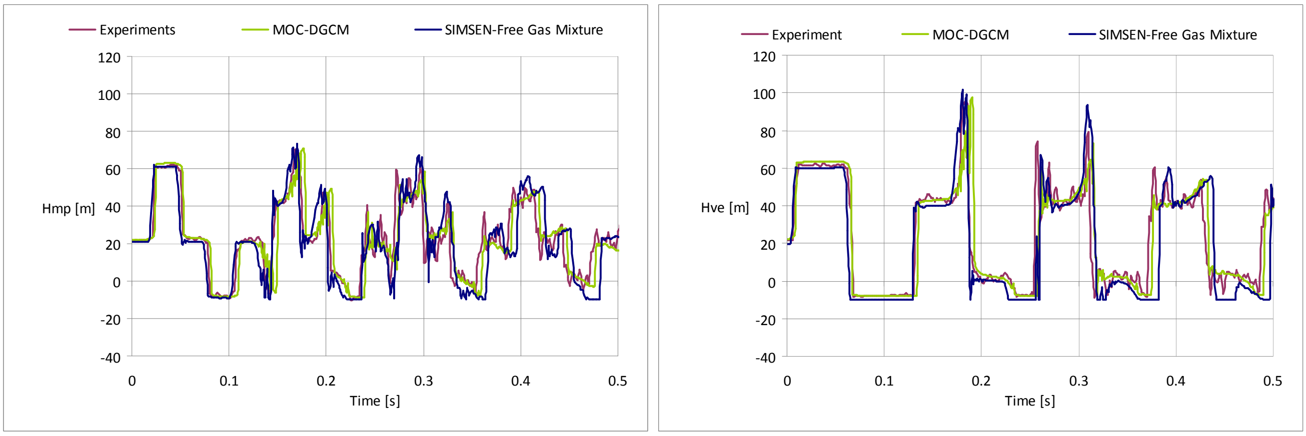

Fig. 10 Comparison simulation results obtained with SIMSEN free-gas mixture model and MOC-DGCM model with experimental results for C_0=0.3 m/s at the midpoint (left) and downstream valve (right)

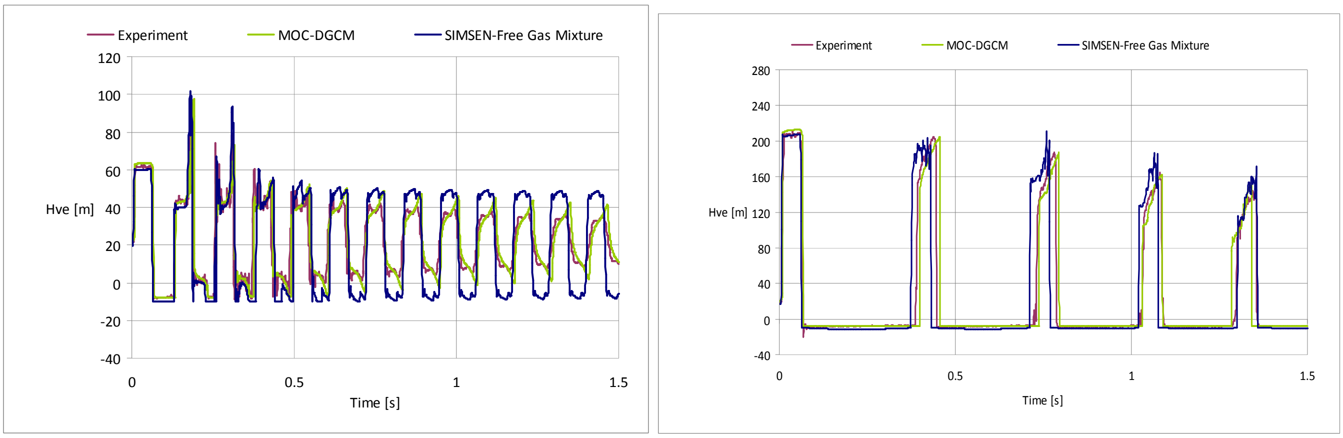

Fig. 11 Comparison simulation results obtained with SIMSEN free-gas mixture model and MOC-DGCM model with experimental at the downstream valve for results for C_0=0.3 m/s (left) and for C_0=1.4m/s (right) over 1.5s

6. Sensitivity analysis of Free Gas Mixture model

The influence of the thermodynamic damping and of the minimum wave speed of the Free Gas Mixture model are pointed out through a sensitivity analysis for the case with initial flow velocity of C_0=1.4m/s by comparing the time evolution at the downstream valve. Simulations are performed with SIMSEN with n=33 elements and a_{min}=20m/s with 3 different values of thermodynamic damping and are compared with experiments in the Fig. 12 left. It can be noticed that as expected the thermodynamic damping influences the damping of the pressure peaks induced by the water column separation and the cavity collapses but also increases the frequency of the collapses. A too low damping leads to an increase of the numerical pressure spikes and after the second pressure peak the pressure is kept to very low values and no more cavity collapse occurs which is obviously not realistic. The simulation results obtained with n=33 elements with a thermodynamic damping of μ''=10^4 Pa·s for three different values of minimum wave speed amin are compared with experiments in Fig. 12 right. It could be noticed that increasing the minimum wave speed to a_{min}=40m/s instead of 20m/s does not affect very much the amplitudes and increases slightly the frequency of the collapses. However, a too low value on minimum wave speeds such as a_{min}=1m/s leads to a large decrease of the frequency of the collapse and leads then to unrealistic pressure amplitudes.

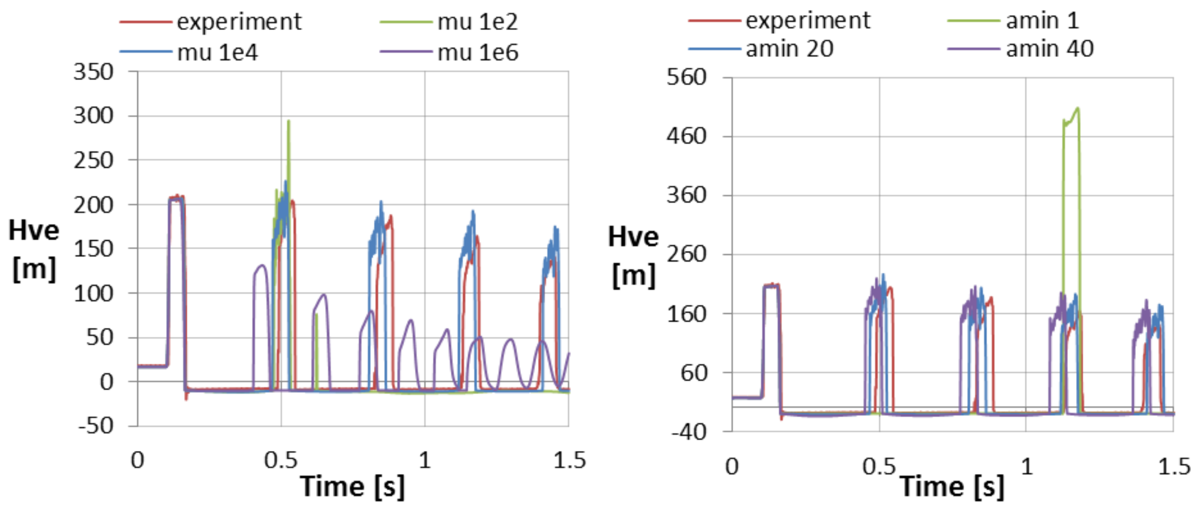

Fig. 12 Comparison simulation results obtained with SIMSEN free-gas mixture model and MOC-DGCM model with experimental at the downstream valve for results for C_0=0.3 m/s (left) and for C_0=1.4m/s (right) over 1.5s

7. Conclusions

A water column separation model based on Free Gas Mixture where the wave speed is function of the pressure and of an initial void fraction and on a thermodynamic damping has been implemented in the SIMSEN simulation software using electrical analogy. Therefore, the equivalent scheme of a cavitation free pressurized pipe is enhanced by introducing the pressure dependency of the wave speed in the capacitance term and by adding a thermodynamic resistance in series with the capacitance to account for energy dissipation related to phase changes. The comparison with experimental results obtained on test rig in case of water hammer induced water column separation shows good agreement if appropriate set of parameters is selected. Indeed, the sensitivity analysis of the thermodynamic damping and of the minimum wave speed shows that too low minimum wave speed and too low damping should be avoided and confirms the order of magnitude of these two parameters. Moreover, the simulation results obtained with the Free Gas Mixture method shows similar agreement as the standard MOC-DGCM model and evidences the role of unsteady friction terms on longer term simulation.

Nomenclature

A	Cross section, m^2	a	Wave speed, m/s
C	Absolute mean flow speed, m/s, $C = Q/A$	h	Piezometric head, $h = Z + p/(\rho g)$, m
D	Pipe diameter, m	l	Length, m
H	Head, m	p	Pressure, Pa.
Q	Flow rate, m^3/s, $Q = C \cdot A$	p_v	Vapor pressure, Pa
R	Hydraulic resistance, s/m^2	g	Gravity acceleration, m/s^2
L	Hydraulic inductance, s^2/m^2	α	Void fraction, -
C	Hydraulic capacitance, m^2	ρ	Water density, kg/m^3
Z	Elevation, m	λ	Friction losses coefficient, -
V_g	Gas volume, m^3	ψ	Weighting factor, -
		dx	Lenth of elementary pipe, m

References

[1] Bergant, A., Simpson, A.R., Tisseling, A.S., 2006, “Water Hammer with Column Separation: A Historical Review”, J. Fluids and Structures, Vol. 22, No. 2, pp. 135-171.

[2] Wylie, E.B., Streeter, V.L., 1993, “Fluid Transients in Systems”. Prentice Hall, Englewood Cliffs, N.J.

[3] Paynter, H.M., 1953 “Surge and Water Hammer Problems”. Transaction of ASCE, Vol. 146, p 962-1009.

[4] Nicolet, C., 2007, “Hydroacoustic Modelling and Numerical Simulation of Unsteady Operation of Hydroelectric Systems”, PhD Thesis, EPFL n°3751, Lausanne, (http://library.epfl.ch/theses/?nr=3751).

[5] Nicolet, C., Alligné, S., Kawkabani, B., Simond, J.-J., Avellan, F., Unstable Operation of Francis Pump-Turbine at Runaway: Rigid and Elastic Water Column Oscillation Modes, Proceedings of the 24th IAHR Symposium on Hydraulic Machinery and Systems, Foz do Iguassu, Brazil, October 27 -31, 2008, paper 150.

[6] Wylie, E.B., 1984, “Simulation of Vaporous and Gaseous Cavitation” J. Fluids Eng., Vol. 106, No0. 3, pp. 307 – 311.

[7] Liou, J.C.P., 2000, “Numerical Properties of the Discrete Gas Cavity Model for Transients”, J. Fluids Eng., Vol. 122, No. 3, pp. 636–639.

[8] Himr, D., Haban, V., 2009, “Simulation of Low Pressure Water Hammer”, Proceedings of the 25th IAHR Symposium on Hydraulic Machinery and Systems, Timisoara, Roumania, September 20-24, paper 1B.3.

[9] Pezzinga, G., 2003, “Second Viscosity in Transient Cavitating Pipe Flows”, J. Hydraulic Research, Vol. 41, No. 6, pp. 656–665.

[10] Alligné, S., Nicolet, C., and Avellan, F., 2011, “Identification of Francis Turbine Helical vortex rope Excitation by CFD and Resonance Simulation with the Hydraulic System,” In Proceedings of ASME-JSME-KSME Joint Fluids Engineering Conference, Hamamatsu, Japan.

[11] Bergant, A., Karadžić, U., Vítkovský, J.P., Vušanović, I., Simpson, A.R., 2005, “A Discrete Gas-Cavity Model that Considers the Frictional Effects of Unsteady Pipe Flow”, J. of Mechanical Eng., Vol. 51, No. 11, pp. 692-710.

[12] Zielke, W., 1968, “Frequency-Dependent Friction in Transient Pipe Flow”, ASME Journal of Basic Engineering, Vol. 90, No. 1, pp. 109-115.

[13] Bergant, A., Simpson, A., R., 1999, “Pipeline Column Separation Flow Regimes”, J. Hydraulic Eng., Vol. 125, No. 8, pp. 835 – 848.